Preclinical Evaluation of New and Highly Potent Analogues of Octreotide for Predictive Imaging and Targeted Radiotherapy

Mihaela Ginj,[1] Jianhua Chen,[1] Martin A. Walter,[1] Veronique Eltschinger,[2] Jean Claude Reubi,[2] and Helmut R. Maecke[1]

[1]Division of Radiological Chemistry, Department of Radiology, University Hospital Basel, Basel, Switzerland and [2]Institute of Pathology, University of Berne, Berne, Switzerland

ABSTRACT

Purpose: **Molecular imaging and targeted radiotherapy are emerging fields in nuclear oncology. Five human somatostatin receptors (hsstr1-hsstr5) are known to be overexpressed to some degree on various tumors, sstr2 being the most important one. Clinically used somatostatin based radiopeptides target exclusively sstr2. The aim of this study was to develop novel analogues with a broader sstr profile for diagnostic (positron emission tomography and single-photon emission computed tomography) and radiotherapeutic applications.**

Experimental Design: **The following promising structures emerged from a parallel synthetic approach: [1,4,7,10-tetraazacyclododecane-1,4,7,10-tetraacetic acid ($DOTA^0$),1-Nal^3,Thr^8]-octreotide (1, DOTA-NOC-ATE) and [$DOTA^0$,$BzThi^3$,Thr^8]-octreotide (2, DOTA-BOC-ATE). The conjugates were labeled with cold and radioactive ^{111}In. Pharmacologic properties were compared with [^{111}In-DOTA,Tyr^3]-octreotide ([^{111}In-DOTA]-TOC).**

Results: **The receptor affinity profile showed high affinity of both peptides to hsstr2, hsstr3, and hsstr5 and some intermediate affinity to hsstr4, whereas [^{111}In-DOTA]-TOC shows affinity only to sstr2. The internalization is fast in sstr2 expressing AR4-2J and in transfected sstr3 expressing human embryonic kidney 293 cells. Both radiopeptides internalize much more efficiently than [^{111}In-DOTA]-TOC. Animal biodistribution studies showed very high and specific uptake of [^{111}In]-1 and [^{111}In]-2 in s.c. implanted AR4-2J tumors (Lewis rats) and in somatostatin receptor expressing normal tissues. The uptake was at least 2-fold higher in these tissues and in the tumor compared with [^{111}In-DOTA]-TOC. In addition, the kidney uptake was significantly lower for both radiopeptides.**

Conclusions: **These data suggest that the novel radiopeptides are superior to [^{111}In/^{90}Y-DOTA]-TOC and show great promise for the clinical application in the imaging of somatostatin receptor–positive tumors and their targeted radiotherapy.**

INTRODUCTION

Targeted radiotherapy using different vector molecules like monoclonal antibodies, peptides, and others has made remarkable progress in recent years. The breakthrough has centered around the first Food and Drug Administration–approved therapeutic radiolabeled monoclonal antibody, Zevalin, an anti-CD20 antibody labeled with ^{90}Y (1). Nevertheless, peptides have several advantages over the antibodies (faster clearance, rapid tissue penetration, no antigenicity, readily synthesized and GMP produced, etc.) and the most commonly used receptor-targeting agents are a variety of somatostatin analogs. The molecular basis for the use of radiolabeled somatostatin analogues in peptide receptor–mediated radionuclide therapy is provided by the overexpression of the five somatostatin receptors (sstr1-sstr5) on a variety of human tumors, especially neuroendocrine tumors and their metastases (2, 3). It is now more than a decade since the first radiolabeled analogue of somatostatin, [^{111}In-diethylentriaminepentaacetic acid (DTPA)]-octreotide (OctreoScan), was approved for scintigraphy of patients with neuroendocrine tumors (4) and it is still one of the best imaging agents (5). Because a β^- particle emitter, such as ^{90}Y, in most cases seems more suitable for tumor therapy (peptide receptor–mediated radionuclide therapy) than the Auger electron emitter ^{111}In, derivatives like 1,4,7,10-tetraazacyclododecane-1,4,7,10-tetraacetic acid (DOTA)-[Tyr^3]-octreotide (DOTA-TOC) have been developed, enabling stable labeling with ^{90}Y, ^{111}In, or ^{177}Lu (6, 7). Numerous preclinical and clinical studies with [^{111}In]- and [^{90}Y]-labeled DOTA-TOC have shown the effective targeting and therapy using these conjugates (7–13). In addition, replacement of the alcohol group at the COOH terminus of the octapeptide by a carboxylic acid group led to increased sstr2 affinity (14, 15) if peptides are labeled with Y^{III}- and Cu^{II}-based radiometals and [^{177}Lu]-[$DOTA^0$,Tyr^3,Thr^8]-octreotide ([^{177}Lu-DOTA]-TATE) showed higher tumor uptake than [^{111}In-DTPA]-octreotide in six patients with somatostatin receptor–positive tumors (16). These new radiopeptides show distinctly higher sstr2 affinity compared with OctreoScan and [In^{III}/Y^{III}-DOTA]-TOC. Nevertheless, they bind with high affinity only to sstr2.

Expression of different somatostatin receptor subtypes in human tumors has been extensively investigated using different methods: mRNA detection [Northern blots (17), *in situ* hybridization (18), RNase protection assays, and reverse transcription-PCR (19)], immunohistochemical studies (20) and receptor autoradiography with subtype-selective ligands (3).

Received 9/7/04; revised 10/26/04; accepted 11/4/04.

Grant support: Swiss National Science Foundation grant 3100A0-100390 (M. Ginj, M. Walter, and H. Maecke) and Bundesamt für Bildung und Wissenschaft grant C00.0091 (M. Ginj and H. Maecke).

The costs of publication of this article were defrayed in part by the payment of page charges. This article must therefore be hereby marked *advertisement* in accordance with 18 U.S.C. Section 1734 solely to indicate this fact.

Note: This work was done within the COST B12 action.

Requests for reprints: Helmut R. Maecke, Division of Radiological Chemistry, Department of Radiology, University Hospital Basel, Petersgraben 4, CH-4031 Basel, Switzerland. Phone: 41-61-265-46-99; Fax: 41-61-265-55-59; E-mail: hmaecke@uhbs.ch.

Although each of these methods has its own disadvantage and the results from all these studies cannot always be compared with each other, they all lead to some common important conclusions. That is, there is a considerable heterogeneity in the expression of individual sstr within and between different tumors, sstr2 being predominantly expressed in a variety of tumors. However, in a significant number of tumors this was being absent or expressed in lower density. For example, correlating immunohistochemical and mRNA detection data with OctreoScan scintigraphy, Papotti et al. (21) found sstr2, sstr3, and sstr5 in human lung tumors. Growth hormone producing adenomas frequently have sstr2 and sstr5; a predominant sstr3 expression has been reported in inactive pituitary adenomas (3, 22) and in thymomas (23); recently, a high incidence of sstr1, sstr2, and sstr3 has been revealed in human cervical and endometrial cancers (24). The expression of sstr1, 2, 3 and 5 is frequently found in gastro-entero-pancreatic tumors (25), medullary thyroid cancers (17) and in epithelial ovarian cancers (26). Therefore, it is obvious that new radiolabeled somatostatin analogues with improved binding affinity profiles are needed.

To extend not only the present range of targeted cancers but also to increase the tumor uptake, given the presence of different receptor subtypes on the same tumor cell or in the same tumor entity, we started a program to design and synthesize radiopeptides with affinity to all sstr. Our strategy was based on two methods: (a) progressive extension of the peptide cycle from octreotide to somatostatin-14 (27) and (b) modification of octreotide. The second approach was realized through parallel solid phase synthesis, mainly by exchanging the amino acids in the positions 3 and 8 of octreotide. We have already reported a first compound resulting from this small library, [^{111}In/^{90}Y-DOTA]-NOC, with improved biological properties, currently in clinical trials (28).

In the present study, we investigated the biological activity profile of two new [^{111}In/In^{III}]-labeled DOTA-peptide conjugates, [DOTA^0,1-Nal^3,Thr^8]-octreotide (**1**, DOTA-NOC-ATE) and [DOTA^0,BzThi^3,Thr^8]-octreotide (**2**, DOTA-BOC-ATE) by means of receptor binding affinity, rate of internalization, cellular retention, and biodistribution in a tumor-bearing rat model. These two compounds are also part of the library acquired through octreotide modification, and their evaluation has been done in comparison with [^{111}In/In^{III}-DOTA]-TOC which in our laboratory is the gold standard of somatostatin receptor imaging and, labeled to ^{90}Y, of targeted radiotherapy.

MATERIALS AND METHODS

All chemicals including 9-fluorenylmethoxycarbonyl–protected amino acids were obtained from commercial sources and used without further purification. Tritylchloride resin was obtained from PepChem (Tübingen, Germany) and $^{111}InCl_3$ from Mallinckrodt Medical (Petten, the Netherlands). The prochelator DOTA(tBu)$_3$ was synthesized according to Heppeler et al. (6). The reactive side chains of the amino acids were masked with one of the following groups: Cys, acetamidomethyl; Lys, *t*-butoxycarbonyl; Thr, *t*-butyl; Trp, *t*-butoxycarbonyl. Analytic reverse phase-high performance liquid chromatography (HPLC) was carried out on a Hewlett-Packard 1050 HPLC system equipped with a multiwavelength detector and a flow-through Berthold LB506C1 γ-detector. Preparative HPLC was done on a Bischof HPLC system (Metrohm AG, Herisau, Switzerland) with HPLC pumps 2250 and a Lambda 1010 UV detector. CC250/4 Nucleosil 120-3C18 columns from Macherey-Nagel (Düren, Germany) were used for analytic HPLC and a VP250/21 Nucleosil 200-5C15 column for preparative HPLC. The gradient systems consisted of mixtures of acetonitrile and water with 0.1% trifluoroacetic acid. Quantitative γ-counting was done on a COBRA 5003 γ-system well counter from Packard Instrument Co. (Hombrechtikon, Switzerland). Electrospray ionization-mass spectrometry was carried out with a Finnigan SSQ 7000 spectrometer (Bremen, Germany).

Synthesis. The peptide-chelator conjugates were synthesized by standard 9-fluorenylmethoxycarbonyl-solid phase synthesis (29) on tritylchloride resin (substitution, 0.8 mmol/g) on a Rink Engineering peptide-synthesizer Switch 24 (RinkCombichem Technologies, Bubendorf, Switzerland) according to the general procedure described previously (28) affording compounds **1** and **2** (Fig. 1), which could be labeled with natural or radioactive indium or yttrium. The compounds were characterized by electrospray ionization-mass spectrometry and reverse phase-HPLC.

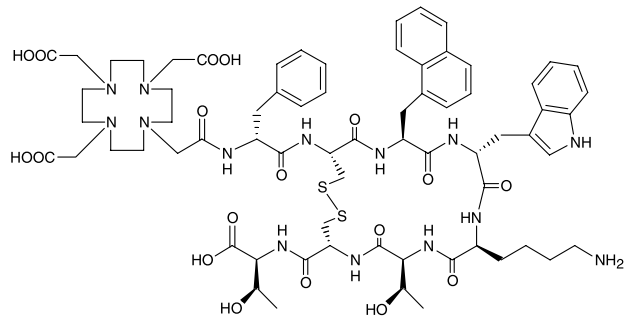

DOTA-NOC-ATE **1**

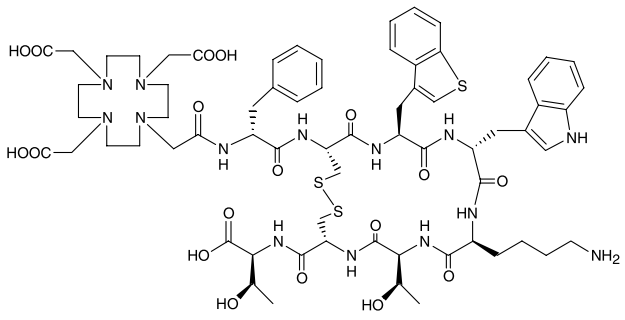

DOTA-BOC-ATE **2**

Fig. 1 Structural formulae of DOTA-[1-Nal^3, Thr^8]-octreotide (DOTA-NOC-ATE, **1**) and DOTA-[BzThi^3, Thr^8]-octreotide (DOTA-BOC-ATE, **2**).

Formation of Metal Complexes. The DOTA-somatotropin release-inhibitingfactor analogues were complexed with $InCl_3$ (anhydrous) and $Y(NO_3)_3{\cdot}5H_2O$ as described by Wild et al. (28). The radiopeptides were also synthesized according to Wild et al. (28) and obtained in >99% radiochemical purity at specific activities of >37 GBq/μmol peptide. For internalization experiments, the DOTA peptides were labeled to a specific activity of about 37 GBq/μmol peptide and then excess $InCl_3$ was added to afford structurally characterized homogenous ligands.

Determination of Somatostatin Receptor Affinity Profiles. CHO-K1 and CCL39 cells stably expressing human sstr1-5 were grown as described previously (14). All culture reagents were supplied by Life Technologies (Grand Island, NY). Cell membrane pellets were prepared and receptor autoradiography was done on pellet sections (mounted on microscope slides), as described in detail previously (14). For each of the tested compounds, complete displacement experiments were done with the universal somatostatin radioligand [^{125}I]-[Leu^8,D-Trp^{22},Tyr^{25}]-somatostatin-28 using increasing concentrations of the Metallo^{III}-DOTA-peptide ranging from 0.1 to 1,000 nmol/L. Somatostatin-28 was run in parallel as control using the same increasing concentrations. IC_{50} values were calculated after quantification of the data using a computer-assisted image processing system. Tissue standards (autoradiographic [^{125}I] microscales, Amersham, Buckinghamshire, United Kingdom) containing known amounts of isotopes, cross-calibrated to tissue-equivalent ligand concentrations, were used for quantification (14). The concentrations of the peptide solutions were measured by UV spectroscopy ($\varepsilon_{NOC\text{-}ATE,\ 280\ nm}$ = 9,855 and $\varepsilon_{BOC\text{-}ATE,\ 280\ nm}$ = 7,570).

Cell Culture, Radioligand Internalization, and Cellular Retention Studies. The AR4-2J cell line was maintained by serial passage in monolayers in DMEM, supplemented with 10% fetal bovine serum, amino acids, vitamins, and penicillin-streptomycin, in a humidified 5% CO_2 atmosphere at 37°C. Human embryonic kidney 293 cells stably expressing rat $sstr_3$ receptors were a gift from Dr. S. Schulz (Magdeburg, Germany; ref. 30) and were grown in DMEM supplemented with 10% fetal bovine serum, penicillin-streptomycin, and G418 (500 μg/mL) in a humidified 5% CO_2 atmosphere at 37°C. Cell numbers were counted under the microscope with a ''Neubauer's counting chamber''. For all cell experiments, the cells were seeded at a density of 0.8 to 1.1 million cells per well in 6-well plates and incubated over night with internalization buffer to obtain a good cell adherence. The loss of cells during the internalization experiments was <10%. When different radiolabeled peptides were compared in cell experiments, the same cell suspension containing plates were used. Furthermore, the internalization rate was linearly corrected to 1 million cells per well in all AR4-2J cell experiments.

Medium was removed from the 6-well plates and cells were washed once with 2 mL of internalization buffer [DMEM, 1% fetal bovine serum, amino acids, and vitamins (pH 7.4)]. Furthermore, 1.5 mL internalization buffer were added to each well and incubated at 37°C for about 1 hour. Thereafter ~500,000 cpm or 0.02 MBq per well ^{111}In/In^{III}-labeled peptides (2.5 pmol per well) to a final concentration of 1.67 nmol/L were added to the medium and the cells were incubated at 37°C for the indicated time periods in triplicates. To determine nonspecific membrane binding and internalization, cells were incubated with radioligand in the presence of 1 μmol/L [In^{III}]-**1**. Cellular uptake was stopped by removing medium from the cells and by washing twice with 1 mL of ice-cold PBS. Acid wash for 10 minutes with a glycine-buffer (pH 2.8) on ice was also done twice. This procedure was done to distinguish between membrane-bound (acid releasable) and internalized (acid resistant) radioligand. Finally, the cells were treated with 1 N NaOH. The culture medium, the receptor bound and the internalized fraction were measured radiometrically in a γ-counter (Packard, Cobra II). Internalization into AR4-2J cells was also studied using three different concentrations of [^{111}In]-**1** and [^{111}In]-2 (6.67 nmol/L or 10 pmol per well, 1.67 nmol/L or 2.5 pmol per well, and 0.167 nmol/L or 0.25 pmol per well).

For cellular retention studies AR4-2J cells (1 million) were incubated with 2.5 pmol per well (1.67 nmol/L) [^{111}In/In^{III}]-labeled DOTA-NOC-ATE, DOTA-BOC-ATE, or DOTA-TOC for 120 and 240 minutes, respectively, then the medium was removed and the wells were washed twice with 1 mL ice-cold PBS. In each experiment, an acid wash for 10 minutes on ice with a glycine-buffer of pH 2.8 was done to remove the receptor-bound ligand. Cells were then incubated again at 37°C with fresh internalization buffer [DMEM containing 1% fetal bovine serum (pH 7.4)]. After different time points, the external medium was removed for quantification of radioactivity in a γ-counter and replaced with fresh 37°C medium. The cells were solubilized in 1 N NaOH, removed and the internalized radioactivity was quantified in a γ-counter. The recycled fraction was expressed as percentage of the total internalized amount per 1 million cells and the integrity of the externalized peptides was determined using HPLC after removing the solvent by a centrifugal evaporator.

Biodistribution and Imaging Studies in Rats. Animals were kept, treated, and cared for in compliance with the guidelines of the Swiss regulations (approval 789). Five-week-old male Lewis rats were implanted s.c. with 10 to 12 millions AR4-2J cells freshly suspended in sterile PBS. Fourteen days after inoculation, the rats showed solid palpable tumor masses (tumor weight, 0.4-0.7 g) and were used for the experiments. Rats were injected under ether anesthesia with 2 to 3 MBq of 0.34 nmol (0.5 μg total peptide mass) [^{111}In]-**1**, [^{111}In]-**2** and [^{111}In-[^{111}In-DOTA]-TOC, respectively, in 0.05 mL NaCl solution 0.9% into the femoral vein. At 4, 24, and 48 hours after injection rats were sacrificed under ether anesthesia. Organs and blood were collected and the radioactivity in these samples was determined using a γ-counter.

To determine the nonspecific uptake of the radiopeptides, rats were injected with 25 μg [In^{III}]-**2** in 0.05 mL NaCl solution 0.9% as a coinjection with the radioligand. To study a potential sstr2, sstr3, and sstr5 related specific uptake of [^{111}In]-**1** in the somatostatin receptor–positive tissues, blocking studies were designed with different somatostatin analogs: DTPA-TATE [sstr2-selective ligand, IC_{50}(sstr2) = 3.9 ± 1 nmol/L], [In^{III}-DTPA]-TATE [sstr2-selective ligand, IC_{50}(sstr2) = 1.3 ± 0.2 nmol/L], and [In^{III}]-2 (sstr2, sstr3, and sstr5 affinity). In a first series, 25 μg of these peptides were coinjected with 2 to 3 MBq

[^{111}In]-1 (0.34 nmol in 0.05 mL NaCl solution 0.9%) into the femoral vein of AR4-2J tumor-bearing male Lewis rats. In a second series, increased amounts of DTPA-TATE (50 μg) and 25 μg of In^{III}-DTPA-TATE were coinjected. Rats were sacrificed at 4 hours and the organs of interest collected and counted for radioactivity. The radioactivity uptake in the tumor and normal tissues of interest was expressed as a percentage of the injected radioactivity dose per gram tissue (% ID/g).

Two rats were used for imaging studies. One rat was injected with 3 MBq of 0.34 nmol [^{111}In]-**1** and the other one was coinjected with the same amount and type of radioligand and 25 μg [In^{III}]-**2** into the femoral vein. Four hours after injection, rats were anaesthetized and images were acquired in the prone position using a γ-camera equipped with a medium energy parallel hole collimator (Basicam, Siemens, Erlangen, Germany).

Statistical Methods. To compare differences between the radiopeptides the Student's *t* test was used.

RESULTS

Synthesis and Labeling. The DOTA-coupled octapeptides **1** and **2** (Fig. 1) were obtained by solid phase synthesis on a tritylchloride resin. The overall yield of the DOTA peptides was about 30%. Uncomplexed and metal-complexed DOTA peptides were characterized by analytic HPLC and electrospray ionization-mass spectrometry. Table 1 lists the calculated and measured molecular weights and also the HPLC retention time of the conjugates and their labeled versions.

Receptor Binding and Affinity Profiles. Table 2 shows the IC_{50} values of the radiopeptides studied in this work as their In^{III} complexed versions in comparison with [In^{III}-DOTA]-TOC for the five somatostatin receptor subtypes. Additionally, the binding profile of the compounds used for the blocking studies in rats are also listed along with the unmodified octapeptides in Table 2. The values were obtained by performing complete displacement experiments with the universal somatostatin radioligand [^{125}I][Leu^{8}, D-Trp^{22}, Tyr^{25}]-somatostatin-28 on membranes from cells expressing the receptor subtypes and were compared with somatostatin-28. All compounds bind specifically to sstr2, with IC_{50} values ranging from 0.8 to 4.6 nmol/L. High binding affinities for sstr3 were found for [In^{III}]-2 (IC_{50} = 5.5 ± 0.8 nmol/L) and [In^{III}]-1 (IC_{50} = 13 ± 4.0 nmol/L), whereas [In^{III}-DOTA]-TOC showed very low sstr3 affinity (IC_{50} = 120 ± 26 nmol/L). [In^{III}]-1 and [In^{III}]-2 displayed moderate affinity for sstr4 (IC_{50} = 160 ± 3.8 and 135 ± 32 nmol/L,respectively).

Table 1 Analytic data of compounds **1**, **2**, [In^{III}]-**1**, and [In^{III}]-**2**

Compound	Calculated MW	Measured MW	RP-HPLC* retention time (min)
DOTA-NOC-ATE, **1**	1,469.68	1,508.2 (M + K^{+})	22.73
DOTA-BOC-ATE, **2**	1,475.71	1,515.4 (M + K^{+})	22.45
[In^{III}-DOTA]-NOC-ATE, [In^{III}]-**1**	1,580.6	1,582.5 (M + H^{+})	23.15
[In^{III}-DOTA]-BOC-ATE, [In^{III}]-**2**	1,587.7	1,589.2 (M + H^{+})	22.9
[In^{III}-DOTA]-TOC	1,533.64	1,534.8 (M + H^{+})	18.23

*Elution system: flow, 0.75 mL/min; solvent A, 0.1% trifluoroacetic acid in H_2O; solvent B, acetonitrile; linear gradient: 0 to 30 minutes, 90% A to 40% A.

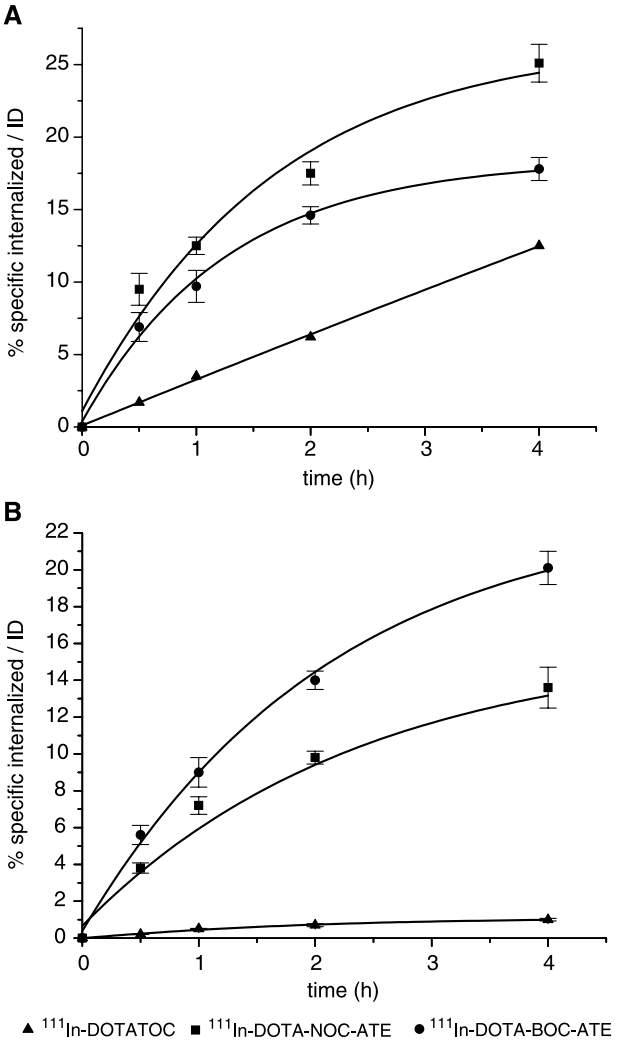

Fig. 2 Comparison of the internalization rate of [^{111}In]-**1**, [^{111}In]-**2**, and [^{111}In-DOTA]-TOC into AR4-2J cells (*A*) and in rsstr$_3$-HEK cells (*B*), respectively. Specific internalization (% dose added to 1 million cells at 1.67 nmol/L concentration) and result of three independent experiments with triplicates in each experiment.

Specific sstr5 affinity was found for [In^{III}]-1 and [In^{III}]-2 (IC_{50} = 4.3 ± 0.5 and 3.9 ± 0.2 nmol/L, respectively).

***In vitro* Internalization Studies in AR4-2J and rsstr3-Human Embryonic Kidney Cells.** Figure 2*A* shows the results of the specific internalization of [^{111}In]-**1** and [^{111}In]-**2** in comparison with [^{111}In-DOTA]-TOC into AR4-2J rat pancreatic tumor cells. The highest rate of internalization corresponds to [^{111}In]-**1** with 25.1 ± 1.3% specific cellular uptake at 4 hours, followed by [^{111}In]-**2** with 17.8 ± 0.8% and [^{111}In-DOTA]-TOC with 12.5 ± 0.7%. The percentage of internalized peptide at 30 minutes as a function of concentration showed a linear dependence (data not shown). Figure 2*B* shows the internalization of [^{111}In]-**1** and [^{111}In]-**2** in sstr3 transfected human embryonic kidney cell lines compared with [^{111}In-DOTA]-TOC. During 4 hours, [^{111}In]-2 internalized 20.1% of the added radiopeptide and [^{111}In]-**1** 13.5%, whereas [^{111}In-DOTA]-TOC showed <0.8% specific internalization.

Table 2 Affinity profiles (IC_{50}) of a series of somatostatin analogues for human somatostatin receptors sstr1 to sstr5

Compound	hsstr1	hsstr2	hsstr3	hsstr4	hsstr5
SS-28	3.6 ± 0.7	2.3 ± 0.6	3.3 ± 0.5	2.7 ± 0.5	2.3 ± 0.3
[In^{III}-DOTA]-NOC-ATE	>10,000	2 ± 0.35	13 ± 4	160 ± 3.8	4.3 ± 0.5
[In^{III}-DOTA]-BOC-ATE	>1,000	1.4 ± 0.37	5.5 ± 0.8	135 ± 32	3.9 ± 0.2
NOC-ATE	>1,000	3.6 ± 1.6	302 ± 137	260 ± 95	16.7 ± 9.9
BOC-ATE	>1,000	0.8 ± 0.4	33 ± 5.5	80 ± 20	3.6 ± 1.5
Octreotide*	>10,000	2.0 ± 0.7	187 ± 55	>10,000	22 ± 6
[In^{III}-DOTA]-TOC*	>10,000	4.6 ± 0.2	120 ± 26	230 ± 82	130 ± 17
DTPA-TATE*	>10,000	3.9 ± 1	>10,000	>1,000	>1,000
[In^{III}-DTPA]-TATE*	>10,000	1.3 ± 0.2	>10,000	433 ± 16	>1,000

NOTE. IC_{50} values are in nmol/L (mean ± SE) and are the mean of at least three experiments. Somatostatin-28 is used as reference.
*Data from Reubi et al. (14).

Cellular Retention. Cellular retention of [^{111}In]-**1,** [^{111}In]-**2** and [^{111}In-DOTA]-TOC was analyzed and compared in AR4-2J cells. In these experiments, the radiopeptides were allowed to internalize for 120 and 240 minutes, respectively; cells were then washed twice with PBS before removing the receptor-bound ligand with glycine buffer (pH 2.8). Warm medium (37°C) was then added and removed after 15, 30, 60, 120, and 240 minutes and measured for radioactivity. Figure 3 illustrates the cellular radioactivity retention of these three compounds in AR4-2J cells over time after two different internalization times. There is no significant difference between the cellular retention after 2 and 4 hours of internalization for the studied conjugates, respectively, except for [^{111}In]-**1** which maintained after 4 hours 30 ± 4.0% ($P < 0.05$) of the 2 hours of internalized fraction and 41.6 ± 6.0% of the 4 hours of internalized fraction, respectively. As shown in Fig. 3, after 4 hours, the percentage of cellular retention for all three conjugates reaches a plateau. HPLC study of the externalized [^{111}In]-**1** and [^{111}In]-**2** gave no indication of metabolites (data not shown).

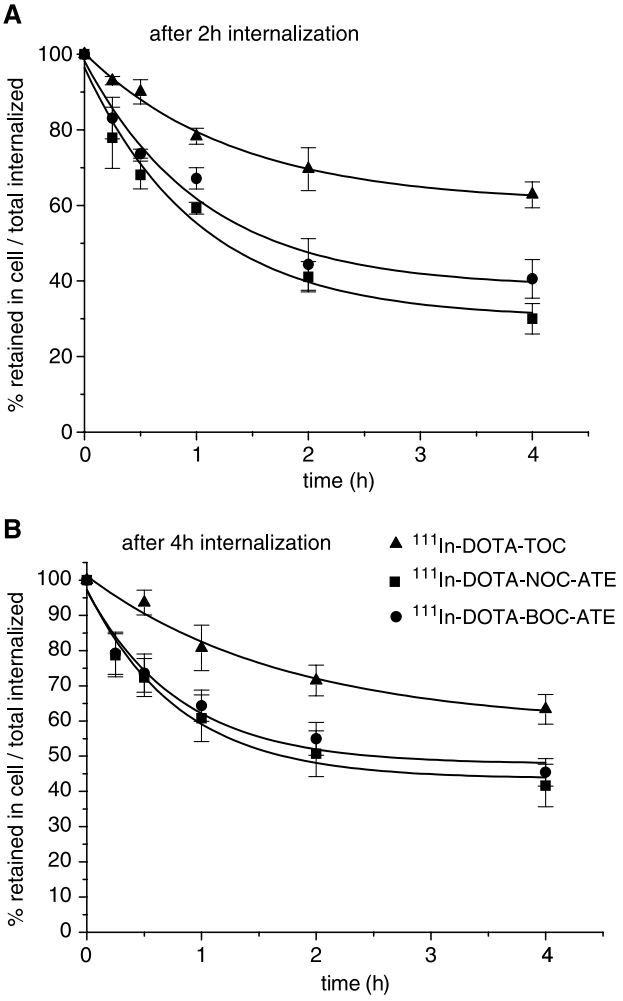

Fig. 3 Comparison of cellular retention over time between[^{111}In]-**1**, [^{111}In]-**2** and [^{111}In-DOTA]-TOC in AR4-2J cells at 37C, after 2 hours of internalization (*A*) and 4 hours of internalization (*B*). % Radioactivity retained in the cell from the total internalized conjugate.

Biodistribution and Imaging Studies in Rats. Pharmacokinetics. The 4, 24, and 48 hours uptake values of [^{111}In]-**1** and [^{111}In]-**2** in somatostatin receptor–positive organs including, pancreas, adrenals, stomach, and AR4-2J rat pancreatic tumor as well as in other tissues are summarized in Table 3. Both radiopeptides displayed rapid blood clearance with <0.04% ID/g remaining in the blood at 4 hours. There is also fast clearance from all sstr-negative tissues except the kidneys which is the main organ of excretion. The two radioligands have a similar biodistribution profile in this rat tumor model except for the adrenals where [^{111}In]-**1** shows a higher uptake than [^{111}In]-**2** (calculated area under the curve: 299.4 versus 164.54% ID/g h). The area under the curve for tumors is 97.2% ID/g h for [^{111}In]-**2** and 95.5% ID/g h for [^{111}In]-**1**, respectively.

Comparison. Figure 4 shows a comparison of the biodistribution properties between [^{111}In]-**1**, [^{111}In]-**2** and [^{111}In-DOTA]-TOC at 4 hours after injection. The tumor uptake for [^{111}In-DOTA]-TOC is 1.95 ± 0.23% ID/g, whereas for [^{111}In]-**1** and [^{111}In]-**2** the values are 4.01 ± 0.49 and 4.12 ± 0.62% ID/g, respectively. Also the uptake in sstr-positive organs (pancreas, adrenals, stomach) is superior for [^{111}In]-**1** and [^{111}In]-**2** (see Table 3) in comparison with [^{111}In-DOTA]-TOC (pancreas, 2.47 ± 0.17% ID/g; adrenals, 1.59 ± 0.16% ID/g; stomach, 0.34 ± 0.02% ID/g). The situation is reversed for the kidney uptake: 2.6 ± 0.12% ID/g for [^{111}In-DOTA]-TOC versus 1.51 ± 0.08% ID/g for [^{111}In]-**1** and 1.79 ± 0.15% ID/g for [^{111}In]-**2**. An evaluation of the tumor-to-different tissues ratios for the three conjugates is presented also in Table 3.

Table 3 Biodistribution in AR4-2J tumor-bearing rats at 4, 24, and 48 hours (n = 4-5 rats per time point) after injection of [^{111}In-DOTA]-NOC-ATE and [^{111}In-DOTA]-BOC-ATE and tissue radioactivity ratios in comparison with [^{111}In-DOTA]-TOC at 4 hours after injection

		[^{111}In-DOTA]-NOC-ATE (%ID/g tissue ± SD)		[^{111}In-DOTA]-BOC-ATE (%ID/g tissue ± SD)	
Organ	Time (h)	Nonblocked	Blocked*	Nonblocked	Blocked*
Blood	4	0.04 ± 0.001	0.014 ± 0.005	0.02 ± 0.003	0.015 ± 0.007
	24	0.004 ± 0.0002		0.005 ± 0.0008	
	48	0.003 ± 0.0001		0.004 ± 0.0002	
Tumor	4	4.01 ± 0.5	0.30 ± 0.03†	4.12 ± 0.62	0.38 ± 0.04†
	24	1.82 ± 0.26		2.04 ± 0.75	
	48	1.11 ± 0.04		1.1 ± 0.17	
Kidneys	4	1.51 ± 0.08	1.56 ± 0.60	1.8 ± 0.15	1.9 ± 0.5
	24	0.74 ± 0.12		1.82 ± 0.16	
	48	0.73 ± 0.07		0.93 ± 0.30	
Adrenals	4	10.75 ± 0.55	0.34 ± 0.03†	5.71 ± 0.53	0.3 ± 0.08†
	24	5.87 ± 1.40		3.34 ± 0.72	
	48	5.22 ± 0.30		2.83 ± 0.63	
Pancreas	4	12.30 ± 0.88	0.32 ± 0.04†	10.33 ± 0.34	0.77 ± 0.03†
	24	2.44 ± 0.30		3.30 ± 0.20	
	48	2.15 ± 0.24		2.52 ± 0.56	
Spleen	4	0.10 ± 0.009	0.04 ± 0.01	0.052 ± 0.005	0.04 ± 0.02
	24	0.03 ± 0.0009		0.048 ± 0.002	
	48	0.03 ± 0.004		0.045 ± 0.01	
Stomach	4	1.83 ± 0.62	0.056 ± 0.001†	0.811 ± 0.22	0.07 ± 0.02†
	24	0.92 ± 0.11		0.65 ± 0.35	
	48	0.41 ± 0.20		0.47 ± 0.06	
Bowel	4	0.25 ± 0.06	0.03 ± 0.01†	0.151 ± 0.023	0.04 ± 0.01†
	24	0.16 ± 0.002		0.13 ± 0.006	
	48	0.14 ± 0.007		0.127 ± 0.001	
Liver	4	0.087 ± 0.05	0.081 ± 0.03	0.095 ± 0.011	0.09 ± 0.02
	24	0.04 ± 0.006		0.067 ± 0.01	
	48	0.038 ± 0.001		0.065 ± 0.01	
Lung	4	0.085 ± 0.008	0.033 ± 0.01†	0.061 ± 0.002	0.04 ± 0.02†
	24	0.02 ± 0.003		0.0445 ± 0.004	
	48	0.018 ± 0.003		0.03 ± 0.0	
Heart	4	0.02 ± 0.001	0.01 ± 0.001	0.013 ± 0.001	0.01 ± 0.005
	24	0.006 ± 0.001		0.008 ± 0.0007	
	48	0.005 ± 0.001		0.008 ± 0.0004	
Bone	4	0.01 ± 0.002	0.01 ± 0.0002	0.012 ± 0.006	0.01 ± 0.005
	24	0.005 ± 0.0009		0.006 ± 0.001	
	48	0.003 ± 0.0007		0.005 ± 0.0004	

Tumor-to-tissue ratios (4 h p.i./24 h p.i.)	[^{111}In-DOTA]-NOC-ATE	[^{111}In-DOTA]-BOC-ATE	[^{111}In-DOTA]-TOC
Tumor/blood	100.3/455	171.6/408	65.5/47.17
Tumor/liver	50.1/45.5	45.7/31	25.8/20.2
Tumor/kidneys	2.7/2.5	2.3/1.12	0.64/0.32

*Blocked with 25 μg [In^{III}-DOTA]-BOC-ATE.
†$P < 0.001$.

Selective Blocking. To estimate the uptake in sstr-positive organs which may be due to receptor subtype expression other than sstr2, *in vivo* blocking studies were done in AR4-2J tumor-bearing rats using different blocking agents like [DTPA^0-Tyr^3-Thr^8]-octreotide (DTPA-TATE) and [In^{III}-DTPA]-TATE, two sstr2-specific ligands and [In^{III}]-**2**, sstr2, sstr3, and sstr5 ligand (see Table 2 for IC_{50} values). Two series of experiments were done, using different amounts of these blocking compounds (Table 4*A* and *B*). As already mentioned in Table 3, 25 μg [In^{III}]-**2** per rat are enough for 95% blocking of the uptake in tumor and sstr-positive organs ($P < 0.001$). Table 4*A* displays the selective blocking of tumor, adrenals, pancreas, and stomach when using only 25 μg DTPA-TATE. As the AR4-2J rat pancreatic tumor expresses only sstr2, the blocking with DTPA-TATE should be as effective as that with [In^{III}]-**2**. In our assay, however, only 70% of the tumor uptake were blocked by the sstr2-selective ligand. In the second selective blocking experiment (Table 4*B*), increased amounts of DTPA-TATE (50 μg per rat) were employed as well as the sstr2-selective ligand [In^{III}-DTPA]-TATE (25 μg per rat) with its improved affinity to this receptor (see Table 2). The two sstr2 ligands were found to be equipotent in decreasing the tumor uptake (85%) but slightly different in their effect on the pancreas and adrenal uptake. The kidney uptake is not influenced by any of these added ligands.

Rat Images. Figure 5 shows the γ-scintigraphy of two Lewis rats s.c. bearing AR4-2J tumors on the thorax 4 hours after injection of [^{111}In]-**1** with (Fig. 5*A*) and without (Fig. 5*B*) coinjection of excess of [In^{III}]-**2**. Coinjection led to a visible

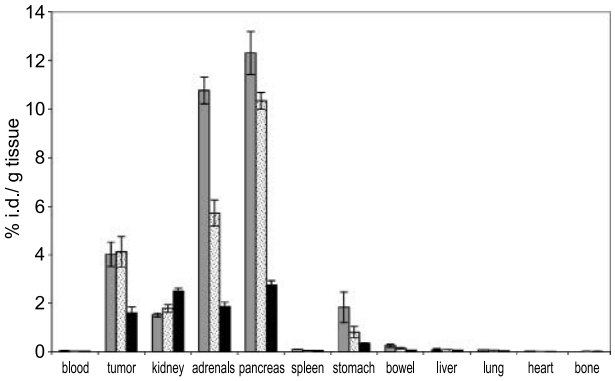

Fig. 4 Biodistribution comparison between [^{111}In-DOTA]-NOC-ATE (▩), [^{111}In-DOTA]-BOC-ATE (▨), and [^{111}In-DOTA]-TOC (■) in AR4-2J tumor-bearing rats at 4 hours after injection.

decrease of the tumor and pancreas uptake, proving the effective blocking of somatostatin receptors. Furthermore, the images show the fast clearance of the radiopeptide from sstr-negative organs and the good target-to-nontarget ratios.

DISCUSSION

This study describes the design, synthesis, and preclinical evaluation of two new somatostatin-based DOTA-coupled peptides for the labeling with a variety of hard acid radiometals like ^{111}In, ^{67,68}Ga, ^{90}Y, and the lanthanides.

The pharmacologic profiles as well as the biological properties of the ^{111}In-labeled peptides are compared with [^{111}In, ^{90}Y-DOTA-Tyr^3]-octreotide (6, 9). The two peptide structures emerged from a parallel synthesis approach with modifications at position 3 of the octapeptide octreotide and the COOH-terminal replacement of Thr(ol) for Thr (14, 15).

The rationale to develop these new peptides came from the desire to develop radiopeptides with a broader spectrum of targeted tumors and a potentially higher uptake in tumors expressing different receptor subtypes concomitantly.

A first radiopeptide emerging from this library of compounds was [^{111}In, ^{90}Y-DOTA]-[1-Nal^3]-octreotide which showed improved affinities towards sstr2, sstr3, and sstr5 if compared with [^{111}In-DOTA]-[Tyr^3]-octreotide (28). The new compounds have several advantages over existing radiopeptides. First, the affinity for sstr2 is as high as the best radiopeptides studied thus far (14). In addition, high affinity to sstr3 and sstr5 was found as well and some emerging sstr4 affinity, thus representing the broadest sstr profile of any somatostatin-based radioligands whereas maintaining a very high sstr2 affinity. The structural features determining the broader affinity profile are not fully understood yet. We observed earlier that the modification of Phe^3 by Tyr^3 in DOTA-coupled octapeptides led to a 3-fold improved sstr2 affinity but the sstr3 affinity dropped by a factor of >10 (14, 28). The higher lipophilicity of benzothienyl-Ala (BzThi) and 1-Nal probably improves sstr3 and sstr5 affinity. The sstr2 affinity increase is most likely a combination of the Thr(ol) versus Thr replacement and the increased lipophilicity at aa^3 position.

A comparison of the affinity profiles of the metallo-chelated peptides with the unmodified peptides BOC-ATE and NOC-ATE showed that BOC-ATE could represent an improved alternative for octreotide (Sandostatin) in the treatment of acromegaly and/or the carcinoid syndrome as it has a higher potency on the receptor subtypes 2-5. Also, the coupling of a DOTA-based metal complex to the N_3-terminus may improve the affinity to some receptor subtypes. [In^{III}-DOTA]-NOC-ATE and [In^{III}-DOTA]-BOC-ATE are at least equipotent to the nonchelated peptide on sstr2 but distinctly more potent on sstr3. On sstr5 [In^{III}-DOTA]-BOC-ATE is equipotent to BOC-ATE but [In^{III}-DOTA]-NOC-ATE is more potent than NOC-ATE.

Somatostatin receptors belong to the family of G-protein coupled receptors (31). There are several important consequences of the coupling of agonists to this type of receptors like desensitization, Ca^{2+} mobilization, cyclic AMP production, and internalization. The latter is of special relevance to the targeting aspects of using G-protein coupled receptor targeting radioligands as it allows long retention times on the tumor which is of special importance in therapeutic applications but may also contribute to the diagnostic sensitivity due to an increased tumor-to-background ratio with time. Both radiopeptides internalize distinctly faster than [^{111}In-DOTA]-TOC in AR4-2J tumor cells. The efflux rate of both radiopeptides from AR4-2J cells is similar, the total amount of cell released radiopeptide is lower if more time is allowed for internalization, indicating that pathways inside the cell slow down the efflux of radiopeptides (32). [^{111}In]-**1** and [^{111}In]-**2** internalize very efficiently into sstr3 cells, [^{111}In]-**2** being clearly superior to [^{111}In]-**1** which may be explained with the higher affinity of [^{111}In]-**2** on sstr3 (see Table 2). [^{111}In-DOTA]-TOC having a

Table 4 Radioactivity uptake in AR4-2J tumor-bearing rats, 4 hours after coinjection of [^{111}In-DOTA]-NOC-ATE and different blocking agents (n = 4 rats per blocking experiment)

Blocking compound	Amount injected per rat (μg)	Radioactivity uptake in organs and tumor (%ID/g tissue ± SD)				
		AR4-2J tumor	Adrenals	Pancreas	Stomach	Kidneys
None		4.01 ± 0.49	10.75 ± 0.55	12.3 ± 0.88	1.83 ± 0.62	1.51 ± 0.08
[InIII-DOTA]-BOC-ATE	25	0.30 ± 0.03*	0.34 ± 0.03*	0.32 ± 0.04*	0.056 ± 0.001*	1.56 ± 0.06*
(A) DTPA-TATE	25	1.26 ± 0.16†	2.13 ± 0.07*	1.85 ± 0.09*	0.24 ± 0.01*	1.57 ± 0.1
(B) DTPA-TATE	50	0.6 ± 0.08*	1.36 ± 0.46*	0.85 ± 0.02*	0.09 ± 0.01*	1.47 ± 0.18
[InIII-DTPA]-TATE	25	0.56 ± 0.07*	0.78 ± 0.11*	0.70 ± 0.09*	0.10 ± 0.02*	1.4 ± 0.29

*$P < 0.001$.
†$0.05 > P > 0.001$ compared with nonblocked data series.

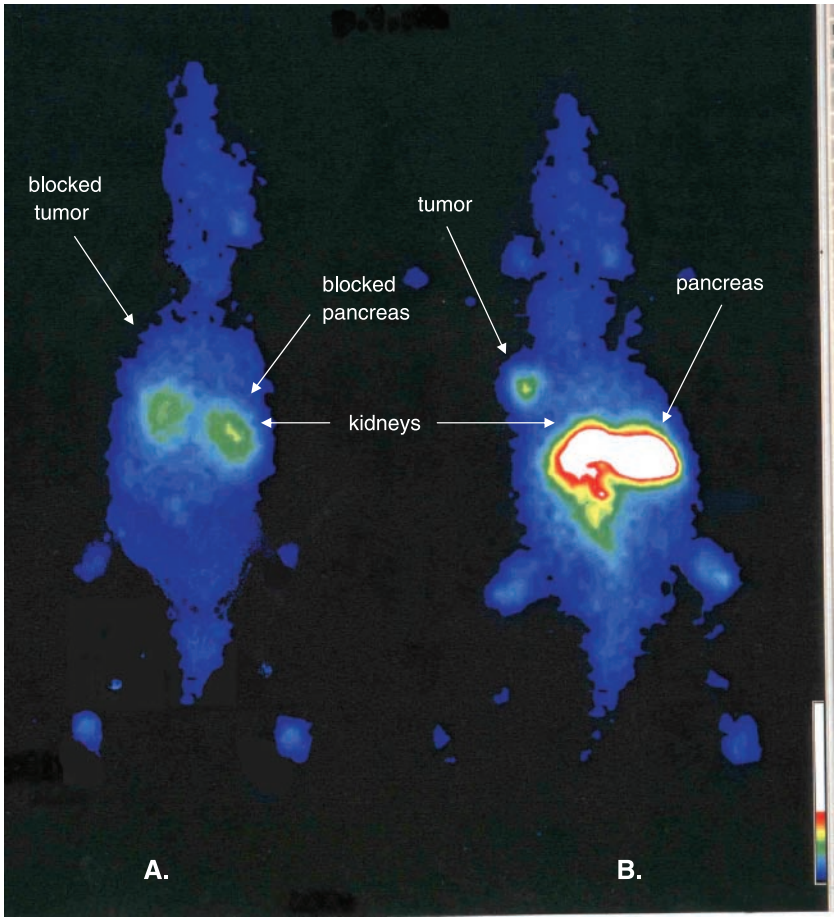

Fig. 5 Four hours post injection scintigraphy of two Lewis rats bearing AR4-2J s.c. tumors: rat with a coinjection of [^{111}In-DOTA]-NOC-ATE and excess [In^{III}-DOTA]-BOC-ATE (*A*) and rat injected only with [^{111}In-DOTA]-NOC-ATE (*B*).

low affinity to sstr3 shows negligible internalization. These data clearly show that [^{111}In]-**1** and [^{111}In]-**2** have a much higher potential to target tumors with sstr3 expression, either alone or concomitantly with other subtypes. The high sstr5 affinity indicates that this also holds for sstr5 expressing tumors.

The efflux rate of the new radiopeptides is faster than the one of [^{111}In-DOTA]-TOC, an effect that we cannot explain at the moment. As the externalized radiopeptides are intact, a faster metabolic degradation cannot be the justification for this. Nevertheless, the amount retained in the cell remains higher for [^{111}In]-**1** and [^{111}In]-**2** than for [^{111}In-DOTA]-TOC, due to the higher internalization rate of the first two. In internalization, we found a close approximation to a steady state after 4 hours of internalization of both new radiopeptides and also the efflux kinetics showed a distinct leveling off after 4 hours. We have explained similar results recently assuming rapid recycling of the radiopeptides to the extracellular medium and reactivation of the receptors by the intact externalized peptides followed by reendocytosis (28). This explanation is also in accordance with the work of Koenig et al. (33).

The *in vivo* pharmacokinetics in the AR4-2J rat model of [^{111}In]-**1** and [^{111}In]-**2** shows a rapid and specific targeting of the somatostatin receptor 2 expressing tumor and somatostatin receptor–positive tissue like the pancreas (Fig. 5*B* for [^{111}In]-**1**). The specificity of this uptake is shown by the blocking experiment which shows lack of uptake in the tumor and the pancreas, even if only 25 μg [In^{III}]-**2** are coinjected with 0.5 μg [^{111}In]-**1** (Fig. 5*A*).

A quantitative analysis of the biodistribution at 4, 24, and 48 hours showed a high uptake in the tumor which was similar for [^{111}In]-**1** and [^{111}In]-**2** but 2-fold higher than for [^{111}In-DOTA]-TOC at 4 hours. The uptake in other somatotropin release-inhibiting factor receptor–positive tissues like the pancreas, adrenals, stomach, and bowel was also very high, specific, and receptor mediated as shown by the blocking experiment. Already a coinjection of 25 μg [In^{III}]-**2** blocks the tumor uptake by >90%, the adrenals by 97%, the pancreas by 95%, the stomach by 97%, and the bowel by 88%, illustrating the potential advantage of the broader affinity profile of this ligand. The almost 7- and 4-fold higher uptake in the adrenals and 5- and 4-fold higher uptake in the pancreas may be explained by the expression of sstr3 and sstr5 in these organs (34). The more efficient blocking capability of [In^{III}]-**2** compared with the sstr2-selective ligands DTPA-octreotate and [In^{III}-DTPA]-octreotate also indicates that this radioligand is superior to other somatostatin-based radiopeptides. The residence time of [^{111}In]-**1** and [^{111}In]-**2** in the tumor is somewhat shorter than that of other somatostatin-based radiopeptides and parallels the efflux rate from AR4-2J cells compared with

[^{111}In-DOTA]-TOC. The area under the curve determining the dose given to the tumor is still very high and justifies diagnostic and therapeutic studies in patients in the near future.

Despite an increased lipophilicity of the new radiopeptides the liver uptake is low and resembles the low uptakes of more hydrophilic radiopeptides like [^{111}In-DTPA-Tyr^3, Thr^8]-octreotide (35) but is much lower than for other hydrophilic radiopeptides like [^{64}Cu-TETA-Tyr^3, Thr^8]-octreotide (15).

Radiometal-labeled peptides show persistent kidney uptake due to proximal tubular cell reabsorption after glomerular filtration, which still makes kidneys the critical organ for therapeutic applications. Both compounds, [^{111}In]-**1** and [^{111}In]-**2** show an improved tumor-to-kidney ratio at all time points which makes these two radiopeptides very promising candidates for somatostatin receptor targeted radiotherapy.

New cold somatostatin-based peptides with superior therapeutic potential and a more universal binding profile than octreotide or lanreotide are currently being developed. Most advanced is SOM230, a cyclohexapeptide that has high binding affinity to sstr1, sstr2, sstr3, sstr5 and is currently under evaluation in phase 1 clinical trials (36). Because there is no radioligand for SOM230, [^{111}In]-**1** and [^{111}In]-**2** may be candidates to identify patients adequate for SOM230 treatment. In addition, [^{111}In]-**1** and [^{111}In]-**2** may be much better alternatives to predict the usefulness of cold octreotide (Sandostatin) or lanreotide (Somatuline) therapy than OctreoScan, which has a much less adequate binding profile for this purpose.

CONCLUSION

We have designed and characterized chemically and pharmacologically two new DOTA-based peptides for diagnostic and therapeutic applications, [^{111}In-DOTA-Nal^3, Thr^8]-octreotide and [^{111}In-DOTA-BzThi^3, Thr^8]-octreotide. The peptides were compared with our clinical gold standard [^{111}In/^{90}Y-DOTA-Tyr^3]-octreotide. They show superior pharmacologic properties when compared with the latter. Both peptides are currently prepared for clinical studies.

The combined preclinical data indicate that [^{111}In, ^{90}Y-DOTA]-NOC-ATE and [^{111}In, ^{90}Y-DOTA]-BOC-ATE are very promising new somatostatin-based radioligands for the diagnosis and targeted radiotherapy of a broader range of tumors expressing somatostatin receptors. They represent the first somatostatin-based radiopeptides, which show high affinity to sstr2, sstr3, and sstr5 and intermediate affinity to sstr4. For the first time, efficient internalization into a sstr3 expressing cell line using radiometallolabeled somatostatin analogues was shown.

We also propose [^{111}In-DOTA]-NOC-ATE and [^{111}In-DOTA]-BOC-ATE as imaging agents to predict the successful use of cold octreotide or lanreotide therapy, as Octreoscan has very low affinity to sstr3 and sstr5.

ACKNOWLEDGMENTS

We thank Dr. S. Schulz for the sstr3-transfected human embryonic kidney 293 cells and Novartis Pharma for the support regarding MS and NMR.

REFERENCES

1. Witzig TE, Gordon LI, Cabanillas F, et al. Randomized controlled trial of yttrium-90-labeled ibritumomab tiuxetan radioimmunotherapy versus rituximab immunotherapy for patients with relapsed or refractory low-grad, follicular, or transformed B-cell non-Hodgkin's Lymphoma. J Clin Oncol 2002;20:2453–63.

2. Reubi JC, Laissue J, Krenning E, Lamberts SW. Somatostatin receptors in human cancer: incidence, characteristics, functional correlates and clinical implications. J Steroid Biochem Mol Biol 1992; 43:27–35.

3. Reubi JC, Waser B, Schaer JC, Laissue JA. Somatostatin receptor sst1-sst5 expression in normal and neoplastic human tissues using receptor autoradiography with subtype-selective ligands. Eur J Nucl Med 2001;28:836–46.

4. Krenning EP, Kwekkeboom DJ, Bakker WH, et al. Somatostatin receptor scintigraphy with [^{111}In-DTPA-D-Phe^1]- and [^{123}I-Tyr^3]-octreotide: the Rotterdam experience with more than 1000 patients. Eur J Nucl Med 1993;20:716–31.

5. Lebtahi R, Le Cloirec J, Houzard C, et al. Detection of neuroendocrine tumors: ^{99m}Tc-P829 scintigraphy compared with ^{111}In-pentetreotide scintigraphy. J Nucl Med 2002;43:889–95.

6. Heppeler A, Froidevaux S, Mäcke HR, et al. Radiometal-labelled macrocyclic chelator-derivatised somatostatin analogue with superb tumour-targeting properties and potential for receptor-mediated internal radiotherapy. Chemistry A European Journal 1999;5:1016–23.

7. de Jong M, Bakker WH, Krenning EP, et al. Yttrium-90 and indium-111 labelling, receptor binding and biodistribution of [DOTA^0, D-Phe^1,Tyr^3]octreotide, a promising somatostatin analogue for radionuclide therapy. Eur J Nucl Med 1997;24:368–71.

8. Otte A, Mueller-Brand J, Dellas S, Nitzsche E, Herrmann R, Maecke H. Yttrium-90-labelled somatostatin-analogue for cancer treatment. Lancet 1998;351:417–8.

9. Waldherr C, Pless M, Maecke H, Haldemann A, Mueller-Brand J. The clinical value of [^{90}Y-DOTA]-D-Phe^1-Tyr^3-octreotide (^{90}Y-DOTATOC) in the treatment of neuroendocrine tumours: a clinical phase II study. Ann Oncol 2001;12:941–5.

10. Cremonesi M, Ferrari M, Zoboli S, et al. Biokinetics and dosimetry in patients administered with ^{111}In-DOTA-Tyr^3-octreotide: implications for internal radiotherapy with ^{90}Y-DOTATOC. Eur J Nucl Med 1999; 26:877–86.

11. Stolz B, Weckbecker G, Smith-Jones PM, Albert R, Raulf F, Bruns C. The somatostatin receptor-targeted radiotherapeutic [^{90}Y-DPTA-DPhe^1,Tyr^3]octreotide (^{90}Y-SMT 487) eradicates experimental rat pancreatic CA 20948 tumours. Eur J Nucl Med 1998;25:668–74.

12. Bushnell D, O'Dorisio T, Menda Y, et al. Evaluating the clinical effectiveness of ^{90}Y-SMT 487 in patients with neuroendocrine tumors. J Nucl Med 2003;44:1556–60.

13. Warner RR, O'Dorisio TM. Radiolabeled peptides in diagnosis and tumor imaging: clinical overview. Semin Nucl Med 2002;32:79–83.

14. Reubi JC, Schar JC, Waser B, et al. Affinity profiles for human somatostatin receptor subtypes SST1-SST5 of somatostatin radiotracers selected for scintigraphic and radiotherapeutic use. Eur J Nucl Med 2000;27:273–82.

15. Lewis JS, Lewis MR, Srinivasan A, Schmidt MA, Wang J, Anderson CJ. Comparison of four ^{64}Cu-labeled somatostatin analogues *in vitro* and in a tumor-bearing rat model: evaluation of new derivatives for positron emission tomography imaging and targeted radiotherapy. J Med Chem 1999;42:1341–7.

16. Kwekkeboom DJ, Bakker WH, Kooij PP, et al. [^{177}Lu-DOTA^{0}-Tyr^3]octreotate: comparison with [^{111}In-DTPA^0]octreotide in patients. Eur J Nucl Med 2001;28:1319–25.

17. Forssell-Aronsson EB, Nilsson O, Bejegard SA, et al. ^{111}In-DTPA-D-Phe^1-octreotide binding and somatostatin receptor subtypes in thyroid tumors. J Nucl Med 2000;41:636–42.

18. Reubi JC, Schaer JC, Waser B, Mengod G. Expression and localization of somatostatin receptor SSTR1, SSTR2, and SSTR3

messenger RNAs in primary human tumors using *in situ* hybridization. Cancer Res 1994;54:3455–9.

19. Buscail L, Saint-Laurent N, Chastre E, et al. Loss of sst2 somatostatin receptor gene expression in human pancreatic and colorectal cancer. Cancer Res 1996;56:1823–7.

20. Reubi JC, Kappeler A, Waser B, Laissue J, Hipkin RW, Schonbrunn A. Immunohistochemical localization of somatostatin receptors sst2A in human tumors. Am J Pathol 1998;153:233–45.

21. Papotti M, Croce S, Bello M, et al. Expression of somatostatin receptor types 2, 3 and 5 in biopsies and surgical specimens of human lung tumours. Correlation with preoperative octreotide scintigraphy. Virchows Arch 2001;439:787–97.

22. Greenman Y, Melmed S. Expression of three somatostatin receptor subtypes in pituitary adenomas: evidence for preferential SSTR5 expression in the mammosomatotroph lineage. J Clin Endocrinol Metab 1994;79:724–9.

23. Ferone D, van Hagen MP, Kwekkeboom DJ, et al. Somatostatin receptor subtypes in human thymoma and inhibition of cell proliferation by octreotide *in vitro*. J Clin Endocrinol Metab 2000;85:1719–26.

24. Schulz S, Schmitt J, Weise W. Frequent expression of immunoreactive somatostatin receptors in cervical and endometrial cancer. Gynecol Oncol 2003;89:385–90.

25. Reubi JC, Waser B. Concomitant expression of several peptide receptors in neuroendocrine tumours: molecular basis for *in vivo* multireceptor tumour targeting. Eur J Nucl Med Mol Imaging 2003;30:781–93.

26. Halmos G, Sun B, Schally AV, Hebert F, Nagy A. Human ovarian cancers express somatostatin receptors. J Clin Endocrinology & Metabolism 2000;85:3509–12.

27. Reubi JC, Eisenwiener KP, Rink H, Waser B, Maecke HR. A new peptidic somatostatin agonist with high affinity to all five somatostatin receptors. Eur J Pharmacol 2002;456:45–9.

28. Wild D, Schmitt JS, Ginj M, et al. DOTA-NOC, a high-affinity ligand of somatostatin receptor subtypes 2, 3 and 5 for labelling with various radiometals. Eur J Nucl Med Mol Imaging 2003;30:1338–47.

29. Atherton E, Sheppard R. Fluorenylmethoxycarbonyl-polyamide solid phase peptide synthesis. General principles and development. In: Solid phase peptide synthesis. A practical approach. Oxford: Oxford Information Press; 1989. p. 25–38.

30. Tulipano G, Stumm R, Pfeiffer M, Kreienkamp HJ, Hollt V, Schulz S. Differential β-arrestin trafficking and endosomal sorting of somatostatin receptor subtypes. J Biol Chem 2004;27:21374–82.

31. Pierce K, Premont R, Lefkowitz R. Seven-transmembrane receptors. Nature Reviews Mol Cell Biol 2002;3:639–50.

32. Wang M, Caruano AL, Lewis MR, Meyer LA, VanderWaal RP, Anderson CJ. Subcellular localization of radiolabeled somatostatin analogues: implications for targeted radiotherapy of cancer. Cancer Res 2003;63:6864–9.

33. Koenig JA, Kaur R, Dodgeon I, Edwardson JM, Humphrey PP. Fates of endocytosed somatostatin sst2 receptors and associated agonists. Biochem J 1998;336:291–8.

34. Raulf F, Perez J, Hoyer D, Bruns C. Differential expression of five somatostatin receptor subtypes, SSTR1-5, in the CNS and peripheral tissue. Digestion 1994;55 Suppl 3:46–53.

35. de Jong M, Breeman WA, Bakker WH, et al. Comparison of ^{111}In-labeled somatostatin analogues for tumor scintigraphy and radionuclide therapy. Cancer Res 1998;58:437–41.

36. Bruns C, Lewis I, Briner U, Meno-Tetang G, Weckbecker G. SOM230: a novel somatostatin peptidomimetic with broad somatotropin release inhibiting factor (SRIF) receptor binding and a unique antisecretory profile. Eur J Endocrinol 2002;146:707–16.